

The swansong in context: long-timescale X-ray variability of NGC 4051

P. Uttley^{1*}, I. M. McHardy¹, I. E. Papadakis², M. Guainazzi³, A. Fruscione⁴

¹*Department of Physics and Astronomy, University of Southampton, Southampton SO17 1BJ*

²*Physics Department, University of Crete, PO Box 2208, 710 03 Heraklion, Crete, Greece*

³*Astrophysics Division, Space Science Department of ESA, ESTEC, Postbus 299, 2200 AG Noordwijk, The Netherlands*

⁴*Harvard-Smithsonian Center for Astrophysics, 60 Garden Street, Cambridge, MA 02138, USA*

Accepted; Received 1999 March 23

ABSTRACT

On 9–11 May 1998, the highly-variable, low luminosity Seyfert 1 galaxy NGC 4051 was observed in an unusual low flux state by *BeppoSAX* (Guainazzi et al. 1998) *RXTE* and *EUVE*. We present fits of the 4–15 keV *RXTE* spectrum and *BeppoSAX* MECS spectrum obtained during this observation, which are consistent with the interpretation that the source had switched off, leaving only the spectrum of pure reflection from distant cold matter. We place this result in context by showing the X-ray lightcurve of NGC 4051 obtained by our *RXTE* monitoring campaign over the past two and a half years, which shows that the low state lasted for ~ 150 days before the May observations (implying that the reflecting material is $> 10^{17}$ cm from the continuum source) and forms part of a lightcurve showing distinct variations in long-term average flux over timescales $>$ months. We show that the long-timescale component to X-ray variability is intrinsic to the primary continuum and is probably distinct from the variability at shorter timescales, possibly associated with variations in the accretion flow of matter onto the central black hole. As the source approaches the low state, the variability process becomes non-linear. NGC 4051 may represent a microcosm of all X-ray variability in radio quiet active galactic nuclei (AGNs), displaying in a few years a variety of flux states and variability properties which more luminous AGNs may pass through on timescales of decades to thousands of years.

Key words: galaxies: active – galaxies: Seyfert – galaxies: NGC 4051 – X-rays: galaxies

1 INTRODUCTION

On 9–11 May 1998, the highly variable, low-luminosity (2–10 keV luminosity, $L_{2-10} \sim 5 \times 10^{41}$ ergs s^{-1}) Seyfert 1 galaxy NGC 4051 was observed in an extremely low, constant flux state (2–10 keV flux $\sim 1.3 \times 10^{-12}$ ergs $cm^{-2} s^{-1}$, corresponding to $L_{2-10} \sim 3 \times 10^{40}$ ergs s^{-1}) by the Rossi X-ray Timing Explorer (*RXTE*), the Italian-Dutch X-ray astronomy satellite *BeppoSAX* and the Extreme Ultraviolet Explorer (*EUVE*). The *BeppoSAX* data were consistent with the interpretation that the source had ‘switched off’, leaving only the X-rays reflected from distant cold matter (possibly the molecular torus) as a witness to its earlier intensity (Guainazzi et al., 1998, henceforth G98).

In this paper, we present the *RXTE* spectrum of the source in its low state, confirming the interpretation presented in G98. We also place this ‘swansong’ of the AGN in

NGC 4051 in context, by showing the two and a half year lightcurve of NGC 4051 obtained with *RXTE*, which shows a decline of the source average flux for nearly two years, culminating in the low state which lasted ~ 150 days before the source ‘switched on’ once more.

Variations on timescales of years, or even on ~ 150 days, in NGC4051 are particularly interesting, given the general pattern of AGN X-ray variability. On short timescales (minutes–hours), AGN such as NGC 4051 display scale invariant variability (e.g. McHardy & Czerny 1987; Lawrence et al. 1987; McHardy 1988; Green, McHardy & Lehto 1993; Lawrence & Papadakis 1993) which can be seen from the power-law shape of their X-ray power spectra. However on longer timescales, $>$ day in the case of NGC4051 (McHardy, Papadakis & Uttley 1998) and $>$ month in the case of the higher luminosity AGNs NGC 5506 (McHardy 1988) and NGC 3516 (Edelson and Nandra 1999), the power spectra flatten, as they must if the total variable power is not to become infinite. Thus the 150 days to few years timescale

* e-mail: pu@astro.soton.ac.uk

which we detect here is much longer than the flattening or ‘knee’ timescale in NGC 4051. In section 5 we discuss this result in the context of the mechanism for the long-timescale X-ray variability and speculate on the implications for other AGN.

2 OBSERVATIONS AND DATA REDUCTION

For the past two and a half years we have monitored NGC 4051 with *RXTE* in order to investigate its variability across a broad range of timescales. To this end, we have used short (< 1 ksec) observations to obtain ‘snapshots’ of the source flux through a range of time intervals. From May 1996 we observed the source twice daily for two weeks, daily for four more weeks and at weekly intervals for the remainder of the year. Since 1997 we have observed the source every two weeks. We also observed NGC 4051 for a continuous period from 1998 May 9 16:43:12 UTC to 1998 May 11 20:55:28 UTC (61 ksec useful exposure), simultaneous with observations by *BeppoSAX* and *EUVE*.

RXTE observed NGC 4051 with the Proportional Counter Array (PCA) and the High Energy X-ray Timing Experiment (HEXTE) instruments. The PCA consists of 5 Xenon-filled Proportional Counter Units (PCUs), sensitive to X-ray energies from 2–60 keV. The HEXTE covers a range of between 20–200 keV, but due to the faint nature of the source we only consider the PCA data in this work. Discharge problems mean that of the 5 PCUs in the PCA, PCUs 3 and 4 are often switched off, so we include data from PCUs 0, 1 and 2 only. We extract data from the top layer of the PCA using the standard *FTOOLS* 4.1 package, using the standard GTI criteria for electron contamination and excluding data obtained within and up to 30 minutes after SAA maximum and data obtained with earth elevation $< 10^\circ$. We estimate the background for the PCA with *PCABACKEST* v2.0C using the new L7 model for faint sources.

3 THE LOW STATE X-RAY SPECTRUM

We now investigate the spectrum of the source in its low state, as measured by the PCA on board *RXTE* and the MECS instrument on *BeppoSAX* during the long-look of May 9–11 1998. The 2–10 keV lightcurve obtained by the PCA shows no significant variability above the expected level for systematic errors in the background estimation, consistent with the observed lack of variability in the *BeppoSAX* lightcurves (G98). We therefore use the PCA and MECS spectra integrated over the whole observation.

We will not consider the data from *EUVE* and the LECS instrument on board *BeppoSAX* in our fits. These data show evidence for a separate low-energy component at energies below 4 keV, in addition to the component seen at medium energies by the PCA and MECS. This low-energy component is also constant in flux over the 7 day duration of the *EUVE* observation (Fruscione, in preparation). Since we are interested in the medium energy spectral component, we shall only consider the PCA and MECS spectra in the energy ranges 4–15 keV and 4–10.5 keV respectively. We use a PCA response matrix generated by the *PCARSP* v2.36 script;

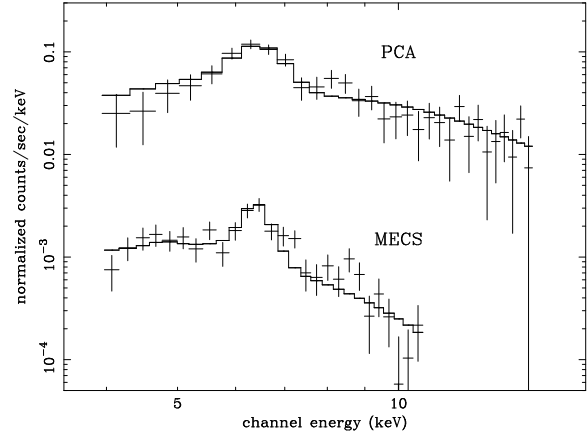


Figure 1. May 9–11 *RXTE* PCA and *BeppoSAX* MECS spectra for the best-fitting multiplicative reflection model described in the text.

details of the MECS calibration and data reduction can be found in G98.

We fit the spectra in *XSPEC* v10.0. Simple power-law fits show a very flat spectrum so, as in G98, we shall attempt to account for this hard spectrum in terms of a reflection model. By fitting up to 15 keV we can use the simple **href** multiplicative model for reflection of a power-law spectrum off a slab of cold material. We also include a gaussian iron line and galactic absorption. This simple model approximates the reflection spectrum of cold material with an unknown distribution around the primary X-ray source. Like G98, we assume that the reflecting material subtends 2π steradians of sky, as seen from the source of the incident continuum. The inclination angle of the reflector to the line of sight is unknown, but since it does not significantly affect the fits, we freeze it arbitrarily at 30 degrees. We find that the best-fitting observed fraction of the illuminating power-law continuum in all our model fits where it is left free is zero (i.e. the source has switched off completely); so we fix this parameter to zero for the purpose of constraining the other model parameters.

In table 1, we show the resulting best-fitting parameters for separate model fits to the PCA and MECS spectra. Both sets of data are fitted reasonably well by the model and the model parameters are consistent with being the same in both the PCA and MECS spectra. The agreement between the two instruments confirms the accuracy of the PCA background model. We therefore attempt to constrain the model parameters further by fitting both the PCA and MECS spectra jointly with the same model parameters. The resulting best-fitting parameters are also shown in table 1.

Fig. 1 shows the model fitted jointly to the spectra from both instruments. The inferred slope of the illuminating continuum, as obtained by the joint fit, is higher than that obtained from the individual fits to both the PCA and MECS spectra. The higher slope is due to the improved definition of the continuum flux at lower energies by the MECS data, which sets the 1 keV continuum normalisation to a higher value than that given by the PCA fit alone, combined with the greater sensitivity of the PCA at high energies which holds down the continuum at higher energies. As one might expect, given that none of the illuminating continuum is di-

Table 1. Best-fitting reflection model parameters for PCA, MECS and combined MECS and PCA spectra.

	Γ	A	E_K	σ_K	F_K	$\chi^2/\text{d.o.f.}$	$L_{2-10}/10^{42} \text{ ergs s}^{-1}$
PCA	$2.1^{+0.4}_{-0.6}$	$(0.6^{+1.0}_{-0.5}) \times 10^{-2}$	$6.42^{+0.18}_{-0.17}$	$0.29^{+0.47}_{-0.29}$	$(2.7^{+2.0}_{-1.1}) \times 10^{-5}$	16.4/26	0.30
MECS	$2.2^{+0.4}_{-0.5}$	$(0.9^{+1.1}_{-0.5}) \times 10^{-2}$	$6.46^{+0.32}_{-0.11}$	$0^{+0.56}_0$	$(1.60^{+1.2}_{-0.6}) \times 10^{-5}$	28.2/22	0.39
PCA & MECS	2.30 ± 0.25	$(1.0^{+0.7}_{-0.3}) \times 10^{-2}$	$6.46^{+0.16}_{-0.09}$	$0.1^{+0.35}_{-0.1}$	$(2.0^{+0.8}_{-0.6}) \times 10^{-5}$	49.0/53	0.38

Γ is the photon index of the incident power-law continuum, A is the incident power-law normalisation, E_K and σ_K are the line energy and actual width respectively (in keV) and F_K is the line flux in photons $\text{cm}^{-2} \text{ s}^{-1}$. All errors are 90% confidence limits for 2 interesting parameters. Also shown is the χ^2 value and number of degrees of freedom for each fit, and the 2–10 keV luminosity of the incident power-law (assuming $H_0 = 50 \text{ km s}^{-1} \text{ Mpc}^{-1}$).

rectly visible, the slope of that continuum is not well determined. However, we note that a continuum photon index of 2.3 was observed during simultaneous *RXTE* and Extreme Ultraviolet Explorer (*EUVE*) observations in May 1996 (Uttley et al., submitted to MNRAS).

The value inferred for the luminosity of the primary continuum incident on the reflector is fairly typical for NGC 4051 in its active state (e.g. Guainazzi et al., 1996). Note that the inferred value for the incident luminosity assumes the slab geometry which is inherent in the reflection model (i.e. 50% covering fraction). Since the inferred continuum luminosity is compatible with observations, the actual covering fraction must be of this order. Fixing the continuum slope of the combined-fit model to its best-fitting value, we can set a 99% confidence upper limit (for 2 interesting parameters) of 0.024 for the fraction of the illuminating primary flux which is directly observed. Combining this observation with the lack of variability from the EUV to medium X-ray bands, the simplest assumption is that the primary continuum has switched off completely.

The iron line parameters are not strongly affected by the parametrization of the underlying continuum. The iron line equivalent width is $\sim 1 \text{ keV}$, consistent with the interpretation that the entire medium-energy spectrum originates in cold reflecting material. The line energy and width are also consistent with this interpretation.

We conclude that the May 1998 long looks at NGC 4051 show that the primary continuum source had switched off for at least seven days leaving the clear signature of reflected emission from cold material, possibly the molecular torus. We will now place this result in context by looking at the source history for the two years preceding these observations and the six months following them.

4 LONG TIMESCALE VARIABILITY

In the upper panel of fig. 2 we show the two and a half year 2–10 keV lightcurve of NGC 4051 obtained with our monitoring observations (crosses). The May long look observation is indicated by a star. The lightcurve shows variability on a range of timescales, including a probable long-term component on timescales of \sim months, which we highlight in the lower panel of fig. 2 which shows the 100 day average fluxes, made with the monitoring data in the corresponding 100 day bins. The error bars on the 100 day averages are intended to represent the spread of points in each bin and do not represent an actual error on the 100 day mean. The lightcurve shows a decline from a high flux state in 1996, through an

intermediate flux state in 1997, culminating in the low state in early 1998 which lasted for ~ 150 days. Shortly after the long-look observations in May 1998 (and as far as the most recent observations) the source became active again.

It is apparent from the lightcurve that the source flux variability is not statistically stationary (i.e. has a constant mean) on long timescales. We now show that this long-term variability is real and not some artifact due to the sparse sampling of an underlying stationary, stochastic lightcurve. We shall use only the monitoring observations since they are all of comparable length and the minimum separation between observations is 0.5 days, which is of the order of the knee timescale. Hence if there are no long-timescale components to variability we would expect any lightcurve made up of such observations to be statistically stationary.

We can compare the mean fluxes of two sections of the lightcurve using Student's t-test for significantly different means (e.g. Press et al., 1992), which gives a probability that both sets of data have the same mean. We first compare the mean 2–10 keV count rate of the 10 observations between TJD 10810 and 10860, (when the source appears to occupy an ultra-low state), with the mean count rate of the preceding 87 observations ($0.92 \text{ counts s}^{-1}$ versus $6.75 \text{ counts s}^{-1}$). The t-test shows that probability that both sets of observations come from the same parent population is 10^{-26} . However, we have selected the group of low-state observations because they look different to the preceding observations. Therefore we must confirm the likelihood that no group of 10 or more consecutive observations can be found to be from the same parent population as a preceding group of observations (with a probability of less than or equal to 10^{-26}), in any randomly generated statistically stationary lightcurve with the same number of data points as our own (106 observations). We have simulated 10^4 statistically stationary lightcurves each with 106 data points. We then searched each simulated lightcurve for groups of 10 or more consecutive points with a mean count rate which is the same as the mean of the preceding points with a probability of 10^{-26} or less. In 10^4 lightcurves we find no such groups, so we conclude that the mean of the lightcurve between TJD 10810 and 10960 is different to the mean in the preceding time period at a level of better than 99.99% confidence. Therefore, the entire lightcurve is not statistically stationary.

We now determine whether the lightcurve is statistically stationary prior to the ultra-low state, i.e. does the source simply switch between two flux states with constant average fluxes, or is there a more gradual change in the mean flux, culminating in the low state? To examine this possibility, we split the lightcurve into two parts of equal dura-

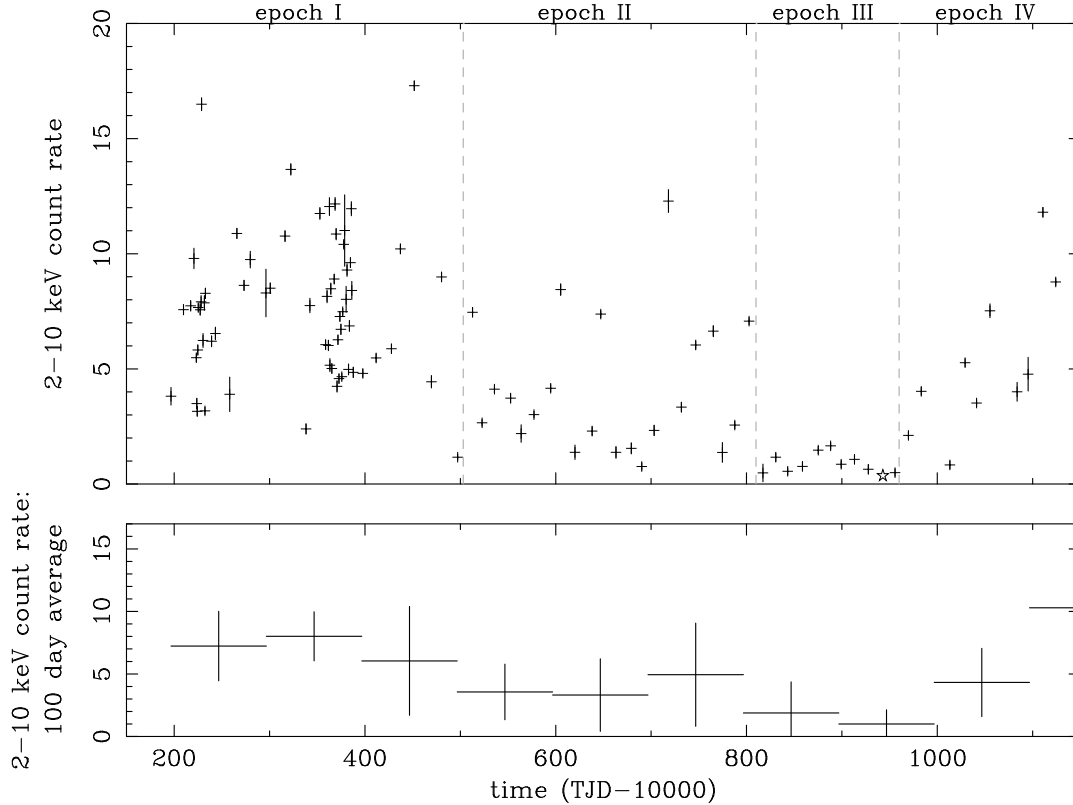


Figure 2. Two and a half year lightcurve of NGC 4051. Errors in the top panel are 1σ counting errors. Errors in the bottom panel are indicative of the spread of points in each 100 day bin. The May 1998 long-look is represented by a star. Time units are Truncated Julian Date (TJD), minus 10^4 for presentation purposes. Grey dashed lines demarcate the epochs described in the text.

tion, corresponding to TJD 10196–10503 and TJD 10503–10810, with mean count rates 7.64 and 4.19 respectively. According to the t-test, these two sections of the lightcurve have significantly different means at better than 99.99% confidence. We cannot show that the lightcurves are not stationary on shorter timescales by further splitting these sections of the lightcurves into equal halves. Therefore the X-ray lightcurve of NGC 4051 approximates a stationary lightcurve on timescales of days–weeks (hence the knee in the power spectrum), becoming non-stationary on longer timescales. We delineate these significantly different flux epochs in Figure 2, naming them epochs I, II, III, and IV. Epoch IV is the most recent section of the lightcurve, where the source seems to have returned to an active state.

Long-term variations in the average X-ray flux might be caused by absorption by a varying column of material along the line of sight. A 50% reduction in average flux (i.e. between epoch I and epoch II) requires an additional absorbing column of column density $\sim 10^{23}$ cm^{-2} , which is ruled out at greater than 99.9% confidence by our spectral data from epoch II observations. Therefore the long-term variations must be intrinsic to the primary X-ray continuum.

Finally, we comment on evidence for non-linearity in the lightcurve. Green, M^cHardy & Done (1999) used the method of searching for asymmetry in the distribution of measured flux about the mean to show that the variability of NGC 4051 was non-linear during a *ROSAT* observation in November 1991, while an observation in November

1992 showed no evidence for non-linearity. Using the same technique, we find that the variability in epoch II is non-linear to 90% confidence although there is no evidence for non-linearity during epoch I (there is not sufficient data to comment on the linearity during the other epochs). It is interesting to note that extrapolating the differing mean X-ray fluxes in epochs I and II into the *ROSAT* band yield *ROSAT* count rates similar to those in November 1992 and November 1991 respectively (assuming a simple power law model with photon index 2.3 and galactic absorption), implying that the non-linear behaviour of NGC 4051 may be associated with the intermediate-flux state which characterises epoch II.

5 DISCUSSION

We now discuss the implications of these results for the interpretation of the low state spectrum and the origin of the long-timescale variability.

Although the source appears to be quiescent during the three days of the May 1998 long-look, there does appear to be some low level of variability during epoch III, although the flux level remains very low, implying that the source may not be entirely switched off for the entire duration of epoch III. The low flux state lasts longer than ~ 150 days, but the reflection spectrum seen in the May 1998 long look, which occurs at the end of the low state, is consistent with reflection of a continuum with much higher flux. We infer that

the reflecting matter lies at distances equal to or greater than ~ 150 light-days from the continuum source ($>$ few times 10^{17} cm), confirming the interpretation of G98 that we have directly detected the X-ray reflection spectrum from the molecular torus in NGC 4051. It is interesting to note that there is no detectable signature of neutral hydrogen gas along the line of sight to the continuum source in NGC 4051, over and above the expected galactic absorption (McHardy et al. 1995), whereas the detection of a reflection spectrum, almost certainly from the surrounding torus, implies substantial columns (greater than 10^{24} cm $^{-2}$) out of the line of sight. This result is in agreement with the standard AGN unification scenario, where we expect substantial differences in the column density along different lines of sight to the central source.

Assuming a lower limit to the timescale for the observed long-term variability of ~ 150 days (i.e., comparable to the duration of the low state) we see that the long-term variability timescale is much longer than the knee timescale in NGC 4051 (by a factor > 50). We therefore speculate that the long timescale component to variability may have an altogether different origin to the variability at much shorter timescales. The short knee timescale of NGC 4051 implies a low black hole mass of order $10^5 M_{\odot}$ if the knee timescale scales linearly with black hole mass (McHardy, Papadakis & Uttley 1998), consistent with the relatively low luminosity of this AGN. The observed long-term variability timescale is much longer than the dynamical timescale for a black hole of this mass, or the thermal or sound-crossing timescales associated with the accretion disk which may fuel the AGN (Edelson & Nandra 1999). However, the long-term variability timescale is comparable with the viscous timescale of an accretion disk (Treves, Maraschi & Abramowicz 1988). We therefore speculate that the long-term X-ray variability of NGC 4051 is related to variations in the accretion flow in the X-ray emitting region close to the massive black hole.

Recently, evidence has emerged for a long timescale component (relative to the knee timescale) to the X-ray variability in the galactic black hole candidate, Cyg X-1 (Rao et al. 1998) on timescales $> 10^3$ s. The long-term variability timescales in Cyg X-1 and NGC 4051 imply a scaling with luminosity (and possibly black hole mass), similar to the scaling with the knee timescale. We therefore speculate that long-term X-ray variability in more luminous AGNs will occur on even longer timescales than in NGC 4051 - from decades to centuries for typical Seyfert galaxies (of $L_X \sim 10^{43}$ ergs s $^{-1}$), to thousands of years for quasars. The X-ray variability of NGC 4051 may represent a microcosm of the X-ray variability of all AGN.

Finally, we note that X-ray experiments with low spectral bandwidth may misclassify sources like NGC 4051, which have recently switched off, as being heavily absorbed AGN.

6 CONCLUSIONS

We have shown that the X-ray spectrum of NGC 4051 in its low state observed by *RXTE* and *BeppoSAX* in May 1998 is consistent with reflection of the primary continuum off distant (> 150 light-days) cold gas, which may be the molecular torus envisaged by the AGN unification model.

We have shown that the X-ray lightcurve of NGC 4051 is not statistically stationary over long timescales, and that during the course of our monitoring campaign, the source does not simply switch between two flux states, but moves from a highly variable (probably linear) high flux state, through an intermediate variable (possibly non-linear) flux state, to the low state where variability was minimal. Since May 1998 the source has become active once more.

The long-timescale component to X-ray variability is intrinsic to the primary continuum (and not varying obscuration), and may be associated with variations in the accretion flow of the putative accretion disk, assuming a relatively small black hole of $10^5 M_{\odot}$, consistent with the low luminosity of this AGN.

The X-ray variability of NGC 4051 may represent a microcosm of all AGN variability, showing in only a few years a range of states and behaviours which more luminous AGN may pass through on timescales of decades to thousands of years.

Acknowledgments

We wish to thank the *RXTE* and *BeppoSAX* schedulers for efficiently co-ordinating and supporting these observations. PU acknowledges financial support from the Particle Physics and Astronomy Research Council, who also provided grant support to IM^cH. MG acknowledges an ESA Research fellowship. AF was supported by *AXAF* Science Center NASA contract NAS 8-39073.

REFERENCES

- Edelson R., Nandra K., 1999, ApJ in press
- Green A. R., McHardy I. M., Done C., 1998, submitted to MNRAS
- Green A. R., McHardy I. M., Lehto H. J., 1993, MNRAS, 265, 664
- Guainazzi M., Mihara T., Otani C., Matsuoka M., 1996, PASJ, 48, 781
- Guainazzi M. et al., 1998, MNRAS, 301, L1
- Lawrence A., Watson M. G., Pounds K. A., Elvis M., 1987, Nat, 325, 694
- Lawrence A., Papadakis I., 1993, ApJ, 414, L85
- McHardy I. M., 1988, MmSAI, 59, 239
- McHardy I. M., Czerny B., 1987, Nat, 325, 696
- McHardy I. M., Green A. R., Done C., Puchnarewicz E. M., Mason K. O., Branduardi-Raymont G., Jones M. H., 1995, MNRAS, 273, 549
- McHardy I. M., Papadakis I. E., Uttley P., 1998, in Scarsi L., Bradt H., Giommi P., Fiore F., eds, Proc. Symp. The active X-ray sky: first results from *BeppoSAX* and *RXTE*. Nucl. Phys. B (Proc. Suppl.), 69/1-3, 509
- Press W. H., Teukolsky S. A., Vetterling W. T., Flannery B. P., 1992, Numerical Recipes, Second edition
- Rao A. R., Agrawal P. C., Paul B., Vahia M. N., Marar T. M. K., Seetha S., Kasturirangan K., 1998, A&A, 330, 181
- Treves A., Maraschi L., Abramowicz M., 1988, PASP, 100, 427

This paper has been produced using the Royal Astronomical Society/Blackwell Science L^AT_EX style file.